Proapoptotic effect of nonthermal pulsed ultrasound on prostate cancer cells in a nude mouse model

Maeda, Koki ; Shigemura, Katsumi ; Hayashi, Fuuka ; Kan, Yuki ; Hiraoka, Aya ; Yamaguchi, Atomu ; Ueda, Minori ; Yang, Yong-Ming ;…

(Citation)
The Prostate,83(12):1217-1226

(Issue Date)
2023-09

(Resource Type)
journal article

(Version)
Accepted Manuscript

Proapoptotic effect of non-thermal pulsed ultrasound on prostate cancer cells in a nude mouse model

Koki Maeda[1], Katsumi Shigemura[1,2], Fuuka Hayashi[2], Yuki Kan[2], Aya Hiraoka[2], Atomu Yamaguchi[3], Minori Ueda[4], Yong-Ming Yang[1], Noriaki Maeshige[3], Tooru Ooya[4,5], Yuzo Nakano[1], Masato Fujisawa[1]

1 Department of Urology, Kobe University Graduate School of Medicine, Kobe, Japan
2 Department of International Health, Kobe University Graduate School of Health Sciences, Kobe, Japan
3 Department of Rehabilitation Science, Kobe University Graduate School of Health Science, Kobe, Japan
4 Department of Chemical Science and Engineering, Graduate School of engineering, Kobe University, Kobe, Japan
5 Center for Advanced Medical Engineering Research & Development (CAMED), Kobe University, Kobe, Japan

Correspondence:
Katsumi Shigemura, MD, PhD
Department of Urology, Kobe University Graduate School of Medicine,
7-5-1 Kusunoki-chou, Chuo-ku, Kobe 650-0017, Japan
Email: katsumi@med.kobe-u.ac.jp

shortened title: Proapoptotic effect of ultrasound

1) data availability statement:

The authors agree to Wiley's data availability when published.

2) funding statement:

The authors did not receive support from any organization for the submitted work.

3) conflict of interest disclosure:

The authors have no conflict of interest to disclose.

4) ethics approval statement:

This animal study was approved by the Ethics Committee of Kobe University.

5) patient consent statement:

Not applicable in this study.

6) permission to reproduce material from other sources:

Not applicable in this study.

7) clinical trial registration:

Not applicable in this study.

Abstract

Background

Ultrasound (US) can induce cell injury, and we have previously reported that adjusting the pulse repetition frequency (PRF) of ultrasound output can induce prostate cancer cell destruction without causing a rise in the temperature of the irradiated area. In this study we examined the mechanism of non-thermal ultrasound cell destruction, which was not fully clarified in our previous reports.

Methods

In vitro, we evaluated post-irradiation cells immediately after treatment and examined membrane disruption by proliferation assay, LDH assay and apoptosis assay. In vivo, we injected mice with human LNCaP and PC-3 prostate cancer cells and evaluated the therapeutic effects of US irradiation by H-E staining and immunostaining.

Results

Proliferation assays showed inhibition at 3 hours post-irradiation independently of PRF and cell line ($p<0.05$). Quantitative assessment of apoptosis/necrosis by flow cytometry showed widely varying results depending on cell type. LNCaP showed an increase in late apoptosis at 0 h independent of PRF ($p<0.05$), while PC-3 showed no significant difference at 0 h. The LDH assay showed an increase in LDH independent of PRF in LNCaP ($p<0.05$ respectively), but no significant difference in PC-3. In vivo, tumor volume was compared and a significant reduction was observed at 10 Hz for LNCaP ($p<0.05$) and 100 Hz for PC-3 ($p<0.001$) at 3 weeks after the start of irradiation. The excised tumors were evaluated with Ki-67, Caspase-3, and CD-31 and showed a significant treatment effect independent of cell type and PRF ($p<0.001$ respectively).

Conclusion

Examining the mechanism behind the therapeutic effect of US irradiation revealed that the main effect was achieved by apoptosis induction rather than necrosis.

Keywords

ultrasound irradiation, prostate cancer,

1. Introduction

Prostate cancer is a very common cancer and the third most common cause of cancer death in men (1). Treatment methods for prostate cancer generally include active surveillance, surgery, radiation therapy, and drug therapy including hormone therapy and anticancer drugs. Each treatment has its advantages and disadvantages. For example, surgery may cause sexual and urinary dysfunction, and radiation may cause urinary obstruction and irritation (2). Less invasive treatments with fewer side effects have been long awaited.

Ultrasound (US) is commonly used for examination and diagnosis and is minimally invasive. It is also widely known that by adjusting the output, it can be used to damage cells (3). HIFU (High Intensity Focused Ultrasound) has been used clinically for prostate cancer therapy. HIFU concentrates high-intensity ultrasound waves to produce thermal and non-thermal effects. The thermal effect produces tissue injury by necrosis and apoptosis (3). HIFU thermal effects have been reported to cause complications such as bladder neck/urethral stricture (4). One of the non-thermal effects is cavitation, where tiny air bubbles are repeatedly generated and collapsed by a brief change in pressure. The bubbles cause damage to cell membranes by creating shock waves in the surrounding area when they vanish (5). The cavitation effects also induce apoptosis and necrosis, the therapeutic effect of US irradiation (3).

We have previously reported that optimizing the pulse repetition frequency (PRF) of non-thermal US has anti-tumor effects on prostate cancer cells (6) and could enhance therapeutic efficacy in a wild type mouse model (7). Our non-thermal US mode has an advantage over HIFU by avoiding treatment risks such as stricture, achieving its anti-tumor effects solely by cavitation. However, we still do not fully understand the

mechanism of the anti-tumor effects and apoptosis/necrosis induced by US irradiation. In particular, US irradiation alone resulted predominantly in apoptosis, but the proportion of necrosis increased in our wild type mouse model where the immune system also attacks the cancer cells (7). To reveal the specific effects of US irradiation on cancer cells, ultrasound has to be applied to cancer cells under immunosuppressive conditions. In this report, we describe the mechanism by which non-thermal US irradiation causes tissue damage in an in vivo experiment using immune-suppressed nude mice and in vitro using a monolayer of prostate cancer cells, focusing on the direct action of US irradiation on the cell membrane and the apoptotic reaction.

2. Materials and Methods

2.1. Cells

To evaluate the therapeutic effects of US irradiation, experiments were performed on two types of human prostate cancer cells. The androgen-dependent LNCaP prostate cancer cell line and the androgen-independent PC-3 prostate cancer cell line were cultured in 35 mm dishes with RPMI-1640 medium (Sigma-Aldrich Japan, Tokyo, Japan) supplemented with10% fetal bovine serum (Sigma-Aldrich, Tokyo, Japan) and 1% penicillin-streptomycin (FUJIFILM Wako Pure Chemical Corporation, Osaka, Japan). Cell cultures were maintained at 37 ºC in a 5% CO2 humidified atmosphere. Cells were seeded at 1.0 x 10^5 squared cells/dish 24 hours prior to irradiation and then irradiated on the following day.

2.2 US Irradiation Treatments

We irradiated LNCaP and PC-3 with US irradiation (3.0W/cm², 3 MHz, irradiation time:

5 minutes, irradiation time rate: 20%) at different PRF of 10 and 100 Hz (a modified model of the SZ-100, MINATO Medical Science, Osaka, Japan). A lower PRF causes a longer pulse and higher PRF causes a shorter pulse per irradiation at the same irradiation time rate. The temperature was kept below 42.5 ºC to avoid thermal necrosis. The observation timing was adjusted for each experimental system.

2.3. Proliferation assay

We performed an MTS assay to evaluate the effects of US irradiation performed at each PRF on the proliferation rate of LNCaP/PC-3. An MTS assay [3-(4,5-dimethylthiazol-2-yl)-5-(3carboxymethoxyphenyl)-2-(4-sulfophenyl)-22H-tetrazolium, inner salt] was performed at two time points, 3 hours and 24 hours after US irradiation. The post-irradiated cells were exposed to MTS for 4 hours and evaluated by measuring absorbance at 490 nm using a spectrophotometer.

2.4. Imaging Assessment of Membrane Damage

We observed live and dead cells using the Cellstain Double Staining Kit (Dojindo Moleculer Technologies, Kumamoto, Japan) and found that US irradiation causes lethal membrane damage. 24 hours after US irradiation, Calcein-AM staining solution and PI staining solution were added at concentrations of 2 μmol/l and 4 μmol/l, respectively, and the cells were incubated for 15 minutes before observation under a fluorescence microscope BZ-X700 (Keyence, Osaka, Japan). Live cells stained green when excited with a filter at 490 nm, and dead cells stained red when excited with a filter at 545 nm.

2.5. Apoptosis/Necrosis Assay

We evaluated the effects of ultrasound-induced membrane damage on the induction of apoptosis and necrosis by flow cytometry. The proportion of apoptotic and necrotic cells was measured by Annexin V and PI dual-staining using the Annexin V-FITC Apoptosis Detection Kit (Nacalai tesque, Kyoto, Japan). The evaluation was conducted at 0 and 24 hours after US irradiation.

2.6. LDH assay

We hypothesized that membrane damage caused by US irradiation is the mechanism of cell destruction, and we performed the Cytotoxicity LDH assay Kit-WST (Dojindo Moleculer Technologies, Kumamoto, Japan) to evaluate the degree of membrane damage observed on cells 24 hours after irradiation.

2.7. Animal Experiments

We conducted animal experiments using nude mice to confirm the antitumor effects of US irradiation on prostate cancer in vivo. All aspects of the experimental design and procedure were reviewed and approved by the institutional ethics and animal welfare committees of Kobe University. Five-week-old Balb/c nu/nu mice were purchased from CLEA Japan, Inc (Tokyo, Japan). 1.0 x 10^6 cells/mice were administrated at day 0 (n = 5, respectively). Fourteen days after administration, tumors reached a long diameter of 7 mm and mice were randomly assigned to 3 groups (Control, PRF:10 Hz, 100 Hz). US irradiation was performed three times a week, and tumor measurement was performed twice a week. Tumor volumes were expressed by the following formula: (longest diameter) × (shortest diameter)^2×0.5. Finally, mice were sacrificed at day 44 and tumors were collected. Tumors were fixed and embedded with paraffin.

172

173 2.8. Immunohistochemical Staining

174 Immunohistochemical (IHC) staining was performed in an automatic tissue processor
175 (Bond-Max, Leica Microsystems, Wetzlar, Germany) following the standard protocol.
176 We evaluated three different antibodies with anti-cleaved Caspase-3 as an apoptosis
177 marker, Ki-67 antibody as a cell proliferation marker, and anti-CD31 primary antibodies
178 as an angiogenesis marker. H–E staining was also performed to assess the necrotic area
179 of the tumor.

180

181 2.9. Immunohistochemical Analysis

182 The stained slides were observed under a microscope BZ-X700 (Keyence, Osaka,
183 Japan). For H–E staining, the ratio of necrotic areas to the entire tumor was calculated.
184 For IHC staining of Ki-67 and Caspase-3, the intensity of staining was evaluated on a
185 4-point scale of 0 (negative), 1 (weak), 2 (intermediate), and 3 (strong), and the range
186 was evaluated on a three-point scale of 1 (0–10%), 2 (11–50%), and 3 (50% or more).
187 The total IHC score was determined by multiplying the frequency and intensity scores
188 (8). For CD-31, the number of stained blood vessels was counted per field of view, and
189 the average of five fields of view was measured.

190

191 2.10. Statistical analysis

192 Comparisons between two different groups were performed using Student's T-test.
193 Comparisons between multiple groups were performed using one-way analysis of
194 variance (ANOVA) followed by the Tukey–Kramer method. Statistical differences
195 among means were considered significant when $p < 0.05$.

3. Results

3.1. Cell proliferation assay (**Figure 1)**

We performed a proliferation assay 3 h and 24 h after US irradiation. At 3 h, both LNCaP and PC-3 showed a significant decrease in viability at 10 Hz and 100 Hz (LNCaP: Ctrl; 1.000, 10Hz; 0.653±0.063 (p=0.043), 100Hz; 0.667±0.071(p=0.015). PC-3: Ctrl; 1.000, 10Hz; 0.808±0.029 (p=0.039), 100Hz; 0.778±0.031(p=0.032)). At 24 hours after US irradiation, only 10 Hz showed a significant difference (LNCaP: Ctrl; 1.000, 10Hz; 0.628±0.096 (p=0.035), 100Hz; 0.938±0.184(p=0.676). PC-3: Ctrl; 1.000, 10Hz; 0.374±0.099 (p=0.020), 100Hz; 0.637±0.010(p=0.056)).

3.2. Imaging Assessment of Membrane Damage **(Figure 2)**

Cells that stain green under a fluorescence microscope are live cells, while cells that stain red are dead cells. The dead cells in the irradiated group show a pale spread of red staining around the cells. Dead cells stain red when the PI stain solution enters the double helix structure of the DNA and turn red, so the spread of staining suggested that cell contents may have been released due to cell membrane damage.

3.3. Apoptosis Assay **(Figure 3)**

The percentages of early apoptosis, late apoptosis, and necrosis were quantified by flow cytometry at 0 and 24 hours after US irradiation, respectively. In LNCaP cells, late apoptosis was significantly increased immediately at 0 hour (10Hz; 8.40±0.68% vs ctrl; 6.07±0.46% (p= 0.040). 100Hz; 11.09±0.64% vs ctrl; 8.49±0.36% (p=0.026)). 24 hours later, only 100 Hz showed a significant difference in apoptosis (early apoptosis 100 Hz,

220 23.61±4.73% vs ctrl 8.06±2.80% (p=0.041); late apoptosis 100Hz 18.03±0.64% vs ctrl
221 9.66±0.23% (p<0.001); total apoptosis 100 Hz 41.64±5.13% vs ctrl 17.71±2.97%
222 (p=0.015)). In PC-3 cells, no significant difference was observed immediately after
223 irradiation at either 10 Hz or 100 Hz, and an increase in late apoptosis and necrosis was
224 only observed at 10 Hz after 24 hours (late apoptosis 10 Hz 11.75±1.13% vs ctrl
225 7.42±0.37% (p=0.020); necrosis 10 Hz 0.20±0.04% vs ctrl 0.02±0.01% (p=0.013)). We
226 performed flow cytometry again with the addition of the apoptosis inhibitor, but the
227 percentage of apoptosis did not decrease and the percentage of necrosis did not increase.
228
229 3.4. LDH assay **(Figure 4)**
230 The LDH kit was used to evaluate the rate at which the cell contents, LDH, were
231 released outside the cell by membrane damage. Prior to the experiment, the cell count
232 was set at 3000 cells/well by measuring high and low controls. Results showed a
233 significant increase in LDH in LNCaP cells at 10 Hz and 100 Hz compared to controls
234 (10 Hz 10.89±0.31% (p<0.001), 100 Hz 2.53±0.27% (p=0.033) vs ctrl 0.14±0.55%).
235 PC-3 showed no significant difference at both 10 Hz and 100 Hz (10 Hz 3.62±0.28%
236 (p=0.531), 100 Hz 2.61±0.53% (p=0.636) vs ctrl 3.10±0.56%).
237
238 3.6. Animal Experiments **(Figure 5)**
239 The therapeutic effect of US irradiation was examined on nude mice transplanted
240 subcutaneously with LNCaP cells and PC-3 cells. Tumor size was significantly reduced
241 by irradiation at 100 Hz for PC-3 and at 10 Hz for LNCaP. Tumors were removed after
242 the final irradiation. LNCaP cells in the 10 Hz group and PC-3 cells in the 100 Hz group
243 were significantly smaller than in the control group (LNCaP: Ctrl, 442.0±166.4 cm^3; 10

Hz, 282.9±58.6 cm^3 (p=0.033);、100 Hz, 339.4±59.7 cm^3 (p=0.167).、PC-3:：Ctrl, 532.8±97.6 cm^3;10 Hz, 443.5±104.2 cm^3 (p=0.109);、100Hz, 313.3±52.1 cm^3 (p<0.001)). In the present study, US irradiation was performed directly on the subcutaneously implanted tumor, and no burns or other side effects were observed on the skin at the irradiated site.

3.7. H-E Staining, Immunohistochemical Staining **(Figures 6, 7)**

The percentage of tumor necrosis was evaluated by HE staining of the excised tissue using the method described above. Both LNCaP and PC-3 showed significant increases in necrotic tissue at 10 Hz and 100 Hz (LNCaP: 10 Hz 16.5±7.3 (p <0.001); 100 Hz, 16.6±6.8 (p <0.001), ctrl, 6.8±1.9; PC-3: 10 Hz, 29.3±9.5 (p <0.001); 100 Hz, 35.8±7.6 (p <0.001); ctrl, 15.0±7.9).

Immunostaining with Ki-67, Caspase-3, and CD31 was then performed. Ki-67 was evaluated as a cell proliferation marker, and Ki-67 expression was significantly suppressed at 100 Hz in both LNCaP and PC-3 compared to the control group (LNCaP: 10 Hz, 6.4±1.8 (p<0.052); 100 Hz, 6.0±1.7 (p<0.002) vs ctrl, 7.1±1.6. PC-3: 10Hz, 5.4±1.8 (p <0.001), 100 Hz, 4.6±1.4 (p <0.001)), vs ctrl, 6.6±1.4). Caspase-3 was evaluated as an apoptosis marker, revealed that while LNCaP results were not significantly different at 10 Hz and 100 Hz, PC-3 was significantly elevated at 10 Hz and 100 Hz compared to the control group (LNCaP: 10 Hz, 4.8±1.0 (p <0.001); 100 Hz, 3.5±1.4 (p <0.001); ctrl 2.3±0.9. PC-3: 10 Hz, 5.7±1.7 (p <0.001); 100 Hz, 5.4±1.5 (p <0.001); ctrl, 3.7±1.5). CD31 was evaluated as a marker of angiogenesis, and LNCaP showed no significant difference, but PC-3 showed significantly suppressed expression at 10 Hz and 100 Hz (LNCaP: 10 Hz, 7.9±2.4 (p <0.001); 100 Hz, 8.4±2.4 (p <0.001);

ctrl 11.4±1.8. PC-3: 10 Hz, 62.8±6.2 ($p < 0.001$); 100 Hz, 43.2±13.4 ($p < 0.001$); ctrl 86.80±9.3).

We observed Differences in sensitivity to US irradiation between LNCaP and PC-3. Especially in vitro, LNCaP showed a significantly greater therapeutic effect than PC-3. On the other hand, in vivo studies have shown similar therapeutic effects in both cases.

4. Discussion

Prostate cancer is the most prevalent malignancy in men and is commonly treated with active surveillance, surgery, radiation, and hormonal therapy. Many cases of localized prostate cancer can be cured by radical surgery or radiotherapy, but surgery has complications such as erectile dysfunction and urinary incontinence, and radiation has complications such as urinary obstruction, irritation and bleeding in the late stages (2). Hormone therapy is effective in many patients, but may eventually lead to castration-resistant prostate cancer (CRPC). Treatment options for CRPC are increasing, but the prognosis is still poor. (9). A less invasive treatment with a different mechanism of action than conventional therapy is much desired.

Ultrasound is commonly used as an examination device, but it is also used for treatment by adjusting the ultrasound output. By varying the power, frequency, and PRF parameters, the ultrasound output produces effects such as tissue injury, apoptosis and necrosis through thermal and non-thermal effects (3). The thermal effects cause tissue injury in various ways including apoptosis, necrosis, altered gene expression, and membrane dysfunction. However, thermal effects may cause irreversible changes to areas other than the target organs of irradiation, and bladder neck/urethral stricture has

been reported as a complication of HIFU (4). The focal area reaches 60 ºC to 85 ºC, causing protein coagulation, fusion of cell membranes, and necrosis of tumor cells. Outside the focal region, the temperature decreases gradually, so the cells are not subjected to immediate death levels of heat, but they are exposed to temperatures above 40 ºC, and most of these cells undergo apoptosis in the days following treatment (10). US irradiation also has non-thermal effects not related to temperature rise. The cavitation effects, one of the mechanisms of non-thermal effects, produce shear forces and pressure changes, release reactive molecules (3) and also induce apoptosis (11).

The US irradiation technology we used in this study produces anti-tumor effects by cavitation, with no thermal effects, by adjusting the ultrasound PRF. Therefore, unlike HIFU, the possibility of urethral stricture or burns due to temperature increase are expected to be reduced in clinical application.

In general, apoptotic cells do not release their cellular constituents into the surrounding interstitial tissue (12), whereas in necrosis the cell membrane is disrupted and cell contents such as nucleus and cytoplasm are released (13). When we observed cells for several hours after irradiation, our findings were suggestive of apoptosis, such as reduction of cellular volume and bleb formation (14), and also were suggestive of necrosis, such as membrane rupture (14) (Fig. 2). In our previous studies using wild type mouse and syngeneic mouse cancer cells, necrosis was the predominant antitumor effect (7). The present study confirmed by flow cytometry that necrosis occurred in only a few cells (Fig. 3), and it was noteworthy that LDH was released extracellularly (Fig. 4). Cell membranes have important function in maintaining cellular homeostasis, and cavitation has a variety of effects on cell membranes depending on the degree of ultrasound pressure. At moderate ultrasound pressure, stable cavitation stimulates

endocytosis. At higher ultrasound pressures, effects become so intense that they pierce the cell membrane, known as sonoporation (15), which is also attracting attention as an intracellular drug delivery method (16). If the pressure is too strong, the damage results in cell death by necrosis (17). US irradiation itself has been shown to induce apoptosis (18), and the mitochondrial caspase pathway and reactive oxygen species are thought to be involved in the mechanism (19). Considering the fact that necrosis is rarely observed while LDH is elevated (Fig 4), our US irradiation mainly resulted in small pore formation in the cell membrane, which induced apoptosis.

The current results show that LNCaP and PC-3 differ in therapeutic efficacy in vitro, specifically that PC-3 may be resistant to treatment compared to LNCaP. This trend has been suggested in previous reports (6). Differences in efficacy by cell type are observed despite the fact that the treatment mechanism is mechanical stimulation, which has also been reported for X-ray radiation (20) and HIFU combined with radiotherapy (21). PC-3 are cells established from bone metastases of CRPC patients, and LNCaP are cells established from lymph node of androgen-dependent prostate cancer patients. A difference in cell membranes may have an impact, as the therapeutic mechanism is the apoptosis-inducing effect of cell membrane disruption.

Not only by cell type, but also by time after US irradiation, the therapeutic effect has been observed to vary. Although the present study was not able to evaluate why there was a difference in therapeutic effect by time, it has been reported that hyperthermia therapy shows cytotoxicity and DNA damage within 24 hours after irradiation, followed by recovery (21). We have observed therapeutic effect in our US irradiation due to the nonthermal effect, but a similar mechanism is expected in terms of mechanical stimulation. Further research is needed.

Although the PRFs that inhibited tumor growth in this animal study differed by cell type, immunohistochemistry staining showed apoptosis-inducing and angiogenesis-inhibiting effects independent of cell type and PRF. PC-3 in particular showed an increase in the area of necrotic tissue, which may have resulted in a greater therapeutic effect than the measured tumor size. PC-3 is an androgen-independent prostate cancer cell difficult to treat in practice, so the possibilities of treatment by US irradiation could be significant.

US irradiation alone in this case was able to inhibit tumor growth, but did not reduce tumor size. It will be necessary to demonstrate a stronger therapeutic effect for clinical use. One way to achieve the stronger effect is in combination with immune checkpoint inhibitors. Prostate cancer is known to be an immunologically "cold" tumor that does not respond well to immune checkpoint inhibitors. However, Eranki et, al. reported that the combination of HUFU and an immune checkpoint inhibitor showed a strong antitumor effect in immunologically "cold" neuroglioma (22). Shibin et al. also reported that the combination of US irradiation and immune checkpoint inhibitors for melanoma in mice showed enhanced antitumor effects and an abscopal effect that was therapeutic even for distant metastases (23). We have also shown that combining US irradiation with a PD-1 antibody enhances the therapeutic effect (7).

Another way to increase the effectiveness of our ultrasound technology would be to create nanobubbles specifically targeted in prostate cancer cells to induce sonoporation through microbubble collapse upon US irradiation (24), which would act more specifically on prostate cancer cells and reduce damage to normal cells. Zlitin et al. reported that creating microbubbles that accumulate in the prostate specific membrane antigen (PSMA) could improve the detection rate of prostate cancer diagnosis by

ultrasound (25). We believe that combining these techniques could potentially improve the therapeutic effect of our US irradiation.

Combining US irradiation with immune checkpoint inhibitors and nanobubbles may have therapeutic potential not only for localized prostate cancer, but also for CRPC with metastases. This US irradiation technology could be applied for prostate cancer treatment in the future, but there are limitations to this study. First, irradiation was performed by applying the probes directly to the tumor subcutaneously. To irradiate the prostate, a transrectal method of irradiation is being considered, and the effects on surrounding normal organs such as the urethra and rectum need to be considered. Second, we used nude mice to examine the therapeutic effect on human prostate cancer cells, so we could not fully evaluate the immunological effects of the treatment. We plan to conduct experiments using mouse prostate cancer cells in the future. Third, in animal studies tumors are removed at the end of treatment, so changes in tumor size after treatment is stopped have not yet been confirmed.

5. Conclusions

The therapeutic effects of non-thermal US irradiation on prostate cancer cells was demonstrated in vitro and in vivo. We also confirmed that the anti-tumor effect of US irradiation is mainly due to the induction of apoptosis.

6. References

1) Siegel RL, Miller KD, Jemal A. Cancer Statistics, 2017. CA Cancer J Clin. 2017 Jan;67(1):7-30.

2) Litwin MS, Tan HJ. The Diagnosis and Treatment of Prostate Cancer: A Review.

JAMA. 2017 Jun 27;317(24):2532-2542.

3) Shankar H, Pagel PS. Potential adverse ultrasound-related biological effects: a critical review. Anesthesiology. 2011 Nov;115(5):1109-24.

4) Poissonnier L, Chapelon JY, Rouvière O, Curiel L, Bouvier R, Martin X, Dubernard JM, Gelet A. Control of prostate cancer by transrectal HIFU in 227 patients. Eur Urol. 2007 Feb;51(2):381-7.

5) Wang X, Ning Z, Lv M, Wu P, Sun C, Liu Y. Transition mechanisms of translational motions of bubbles in an ultrasonic field. Ultrason Sonochem. 2023 Jan;92:106271.

6) Maeshige N, Kitagawa K, Yamasaki S, Ishii A, Shirakawa T, Yang YM, Sung SY, Chen KC, Yuan ZM, Shigemura K, Fujisawa M. Can ultrasound irradiation be a therapeutic option for prostate cancer? Prostate. 2020 Sep;80(12):986-992.

7) Hayashi F, Shigemura K, Maeda K, Hiraoka A, Maeshige N, Ooya T, Sung SY, Yang YM, Fujisawa M. Combined Treatment with Ultrasound and Immune Checkpoint Inhibitors for Prostate Cancer. J Clin Med. 2022 Apr 27;11(9):2448.

8）Yamamichi F, Shigemura K, Behnsawy HM, Meligy FY, Huang WC, Li X, Yamanaka K, Hanioka K, Miyake H, Tanaka K, Kawabata M, Shirakawa T, Fujisawa M. Sonic hedgehog and androgen signaling in tumor and stromal compartments drives epithelial-mesenchymal transition in prostate cancer. Scand J Urol. 2014 Dec;48(6):523-32.

9) Terada N, Sawada A, Kawanishi H, Fujimoto T, Magaribuchi T, Chihara I, Hashimoto K, Sakurai T, Shimizu Y, Uegaki M, Nakashima M, Narita S, Kubota M, Yamada Y, Tohi Y, Okabe K, Yatsuda J, Kamoto T. The efficacy of sequential therapy with docetaxel and cabazitaxel for castration-resistant prostate cancer: A retrospective multi-institutional study in Japan. Int J Urol. 2022 Nov 14.

412 10) Hoogenboom M, Eikelenboom D, den Brok MH, Veltien A, Wassink M, Wesseling
413 P, Dumont E, Fütterer JJ, Adema GJ, Heerschap A. In vivo MR guided boiling
414 histotripsy in a mouse tumor model evaluated by MRI and histopathology. NMR
415 Biomed. 2016 Jun;29(6):721-31.
416 11) Stanton MT, Ettarh R, Arango D, Tonra M, Brennan PC. Diagnostic ultrasound
417 induces change within numbers of cryptal mitotic and apoptotic cells in small
418 intestine. Life Sci. 2001 Feb 16;68(13):1471-5.
419 12) Elmore S. Apoptosis: a review of programmed cell death. Toxicol Pathol. 2007
420 Jun;35(4):495-516.
421 13) Vandenabeele P, Galluzzi L, Vanden Berghe T, Kroemer G. Molecular mechanisms
422 of necroptosis: an ordered cellular explosion. Nat Rev Mol Cell Biol. 2010
423 Oct;11(10):700-14.
424 14) Kroemer G, Galluzzi L, Vandenabeele P, Abrams J, Alnemri ES, Baehrecke EH,
425 Blagosklonny MV, El-Deiry WS, Golstein P, Green DR, Hengartner M, Knight RA,
426 Kumar S, Lipton SA, Malorni W, Nuñez G, Peter ME, Tschopp J, Yuan J, Piacentini
427 M, Zhivotovsky B, Melino G; Nomenclature Committee on Cell Death 2009.
428 Classification of cell death: recommendations of the Nomenclature Committee on
429 Cell Death 2009. Cell Death Differ. 2009 Jan;16(1):3-11.
430 15) Kooiman K, Roovers S, Langeveld SAG, Kleven RT, Dewitte H, O'Reilly MA,
431 Escoffre JM, Bouakaz A, Verweij MD, Hynynen K, Lentacker I, Stride E, Holland
432 CK. Ultrasound-Responsive Cavitation Nuclei for Therapy and Drug Delivery.
433 Ultrasound Med Biol. 2020 Jun;46(6):1296-1325.
434 16) Deprez J, Lajoinie G, Engelen Y, De Smedt SC, Lentacker I. Opening doors with
435 ultrasound and microbubbles: Beating biological barriers to promote drug delivery.

436 Adv Drug Deliv Rev. 2021 May;172:9-36.
437 17) Prentice, P., Cuschieri, A., Dholakia, K., Mark Prausnitz, Paul Campbell. Membrane
438 disruption by optically controlled microbubble cavitation. *Nature Phys* 1, 107–110
439 (2005).
440 18) Ashush H, Rozenszajn LA, Blass M, Barda-Saad M, Azimov D, Radnay J, Zipori D,
441 Rosenschein U. Apoptosis induction of human myeloid leukemic cells by ultrasound
442 exposure. Cancer Res. 2000 Feb 15;60(4):1014-20.
443 19) Honda H, Kondo T, Zhao QL, Feril LB Jr, Kitagawa H. Role of intracellular
444 calcium ions and reactive oxygen species in apoptosis induced by ultrasound.
445 Ultrasound Med Biol. 2004 May;30(5):683-92.
446 20）Adamczuk GM, Humeniuk E, Adamczuk K, Madej-Czerwonka B, Dudka J.
447 Disruption of mitochondrial function augments the radiosensitivity of prostate cancer
448 cell lines. Ann Agric Environ Med. 2023 Mar 31;30(1):65-76.
449 21) Zhang X, Bobeica M, Unger M, Bednarz A, Gerold B, Patties I, Melzer A, Landgraf
450 L. Focused ultrasound radiosensitizes human cancer cells by enhancement of DNA
451 damage. Strahlenther Onkol. 2021. Aug; 197(8):730-743.
452 22) Eranki A, Srinivasan P, Ries M, Kim A, Lazarski CA, Rossi CT, Khokhlova TD,
453 Wilson E, Knoblach SM, Sharma KV, Wood BJ, Moonen C, Sandler AD, Kim PCW.
454 High-Intensity Focused Ultrasound (HIFU) Triggers Immune Sensitization of
455 Refractory Murine Neuroblastoma to Checkpoint Inhibitor Therapy. Clin Cancer Res.
456 2020 Mar 1;26(5):1152-1161.
457 23) Qu S, Worlikar T, Felsted AE, Ganguly A, Beems MV, Hubbard R, Pepple AL,
458 Kevelin AA, Garavaglia H, Dib J, Toma M, Huang H, Tsung A, Xu Z, Cho CS.
459 Non-thermal histotripsy tumor ablation promotes abscopal immune responses that

enhance cancer immunotherapy. J Immunother Cancer. 2020 Jan;8(1).

24）Chen X, Leow RS, Hu Y, Wan JM, Yu AC. Single-site sonoporation disrupts actin cytoskeleton organization. J R Soc Interface. 2014 Mar 26;11(95):20140071.

25）Zlitni A, Yin M, Janzen N, Chatterjee S, Lisok A, Gabrielson KL, Nimmagadda S, Pomper MG, Foster FS, Valliant JF. Development of prostate specific membrane antigen targeted ultrasound microbubbles using bioorthogonal chemistry. PLoS One. 2017 May 4;12(5):e0176958.

7. Figure Legends

Figure 1. Proliferation assay

Proliferation assays were performed at 3 and 24 hours after US irradiation. After 3 hours of irradiation, both LNCaP and PC-3 showed significant differences at 10 Hz and 100 Hz (all p-values < 0.05), but after 24 hours of irradiation, only 10 Hz showed significant differences (LNCaP: 10 Hz $p=0.035$, 100 Hz $p=0.676$. PC-3: 10 Hz $p=0.020$, 100 Hz $p=0.056$).

Figure 2. Imaging Assessment of Membrane Damage

Double staining, with live cells stained green and dead cells stained red, was used to evaluate membrane disruption caused by US irradiation, using a fluorescence microscope at 40x zoom.

In both LNCaP cells (Fig A) and PC-3 cells (Fig B), the red stain spread around the dead cells in the irradiated group. The red color fluoresces in response to DNA, indicating that cell contents may have been released around the dead cells.

Figure 3. Apoptosis Assay

To explore the anti-tumor mechanism of US irradiation, the percent of apoptosis and necrosis was quantitatively evaluated by flow cytometry. Results showed that the percentage of necrosis was very limited and apoptosis was predominant. Especially in LNCaP (A), an increase in late apoptosis was observed immediately after irradiation, and at 24 hours a significant increase was observed at 100 Hz for early apoptosis, late apoptosis, and total apoptosis.

Figure 4. LDH assay

LDH assays were used to confirm that US irradiation disrupts cell membranes and releases cell contents. In LNCaP, LDH was predominantly increased compared to controls (10 Hz: $p<0.001$, 100 Hz: $p=0.033$), but no significant difference was observed in PC-3 regardless of PRF.

Figure 5. Animal Experiment

(A) LNCaP and PC-3 were subcutaneously implanted in mice and US irradiation was performed three times a week starting 14 days after administration when tumor diameters reached 7 mm. Tumor size measurements were performed twice a week.

(B) Figure shows the change in tumor size over time with treatment, with LNCaP showing a significant difference at 10 Hz compared to controls ($p=0.033$) and PC-3 showing a significant difference at 100 Hz compared to controls ($p<0.001$).

Figure 6. H-E stain

H-E staining was performed on excised tumor cells and the areas of necrotic tissue were analyzed for comparison. Although the comparison of tumor size showed significant differences at 10 Hz for LNCaP and 100 Hz for PC-3, the area of necrotic tissue was significantly increased in H-E staining, independent of PRF ($p<0.001$, respectively).

Figure 7. Immunohistochemical analysis

Three types of immunohistochemistry staining were performed on the excised tumors. Ki-67 expression, as a cell proliferation marker, showed proliferation was significantly suppressed at 100 Hz in both LNCaP and PC-3 and 10 Hz in PC-3. Caspase-3 expression, as an apoptosis marker, was significantly elevated in both LNCaP and PC-3 independent of PRF. CD31 expression, as a marker of angiogenesis, was also significantly suppressed in both LNCaP and PC-3 independent of PRF.

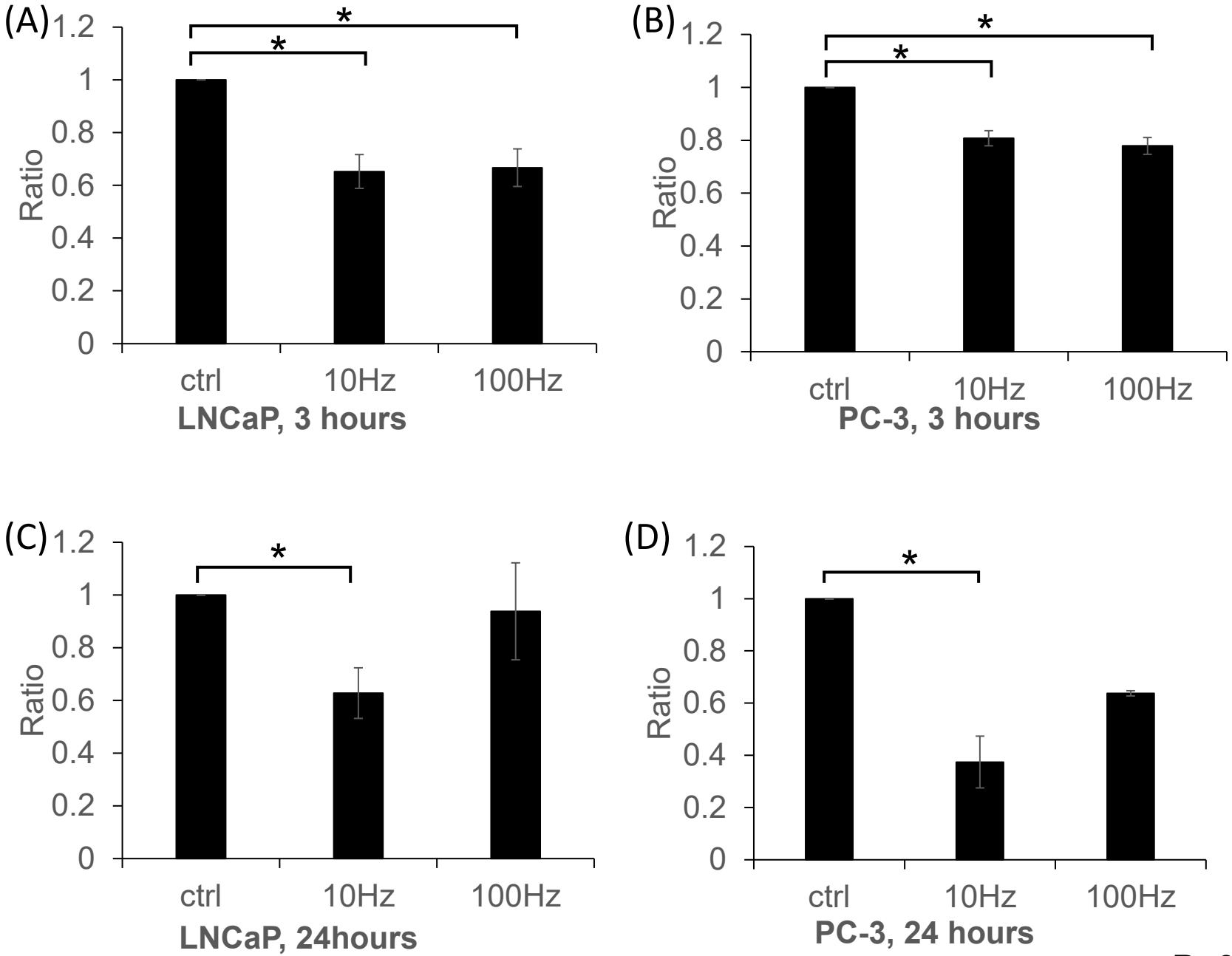
(A)
1.2
1
0.8
0.6
0.4
0.2
0
Ratio
*
*
ctrl
10Hz
100Hz
LNCaP, 3 hours
(B)
1.2
1
0.8
0.6
0.4
0.2
0
Ratio
*
*
ctrl
10Hz
100Hz
PC-3, 3 hours
(C)
1.2
1
0.8
0.6
0.4
0.2
0
Ratio
*
ctrl
10Hz
100Hz
LNCaP, 24hours
(D)
1.2
1
0.8
0.6
0.4
0.2
0
Ratio
*
ctrl
10Hz
100Hz
PC-3, 24 hours
*:P<0.05

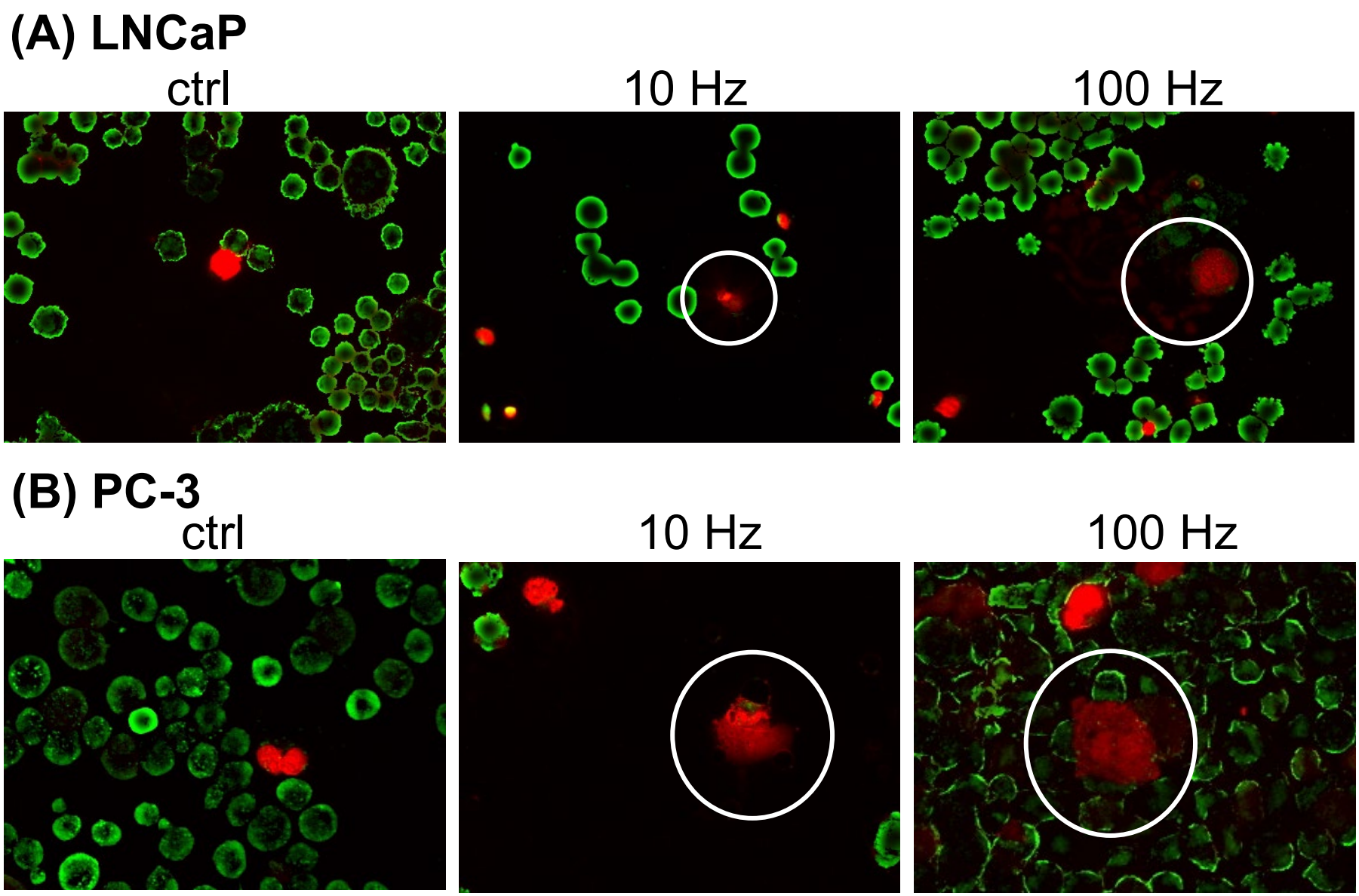
(A) LNCaP
ctrl
10 Hz
100 Hz
(B) PC-3
ctrl
10 Hz
100 Hz

(A) LNCaP

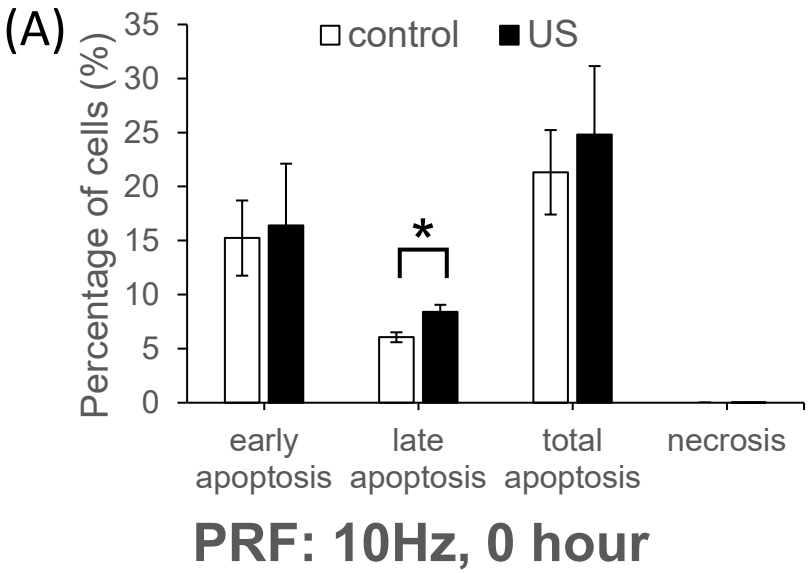

PRF: 10Hz, 0 hour

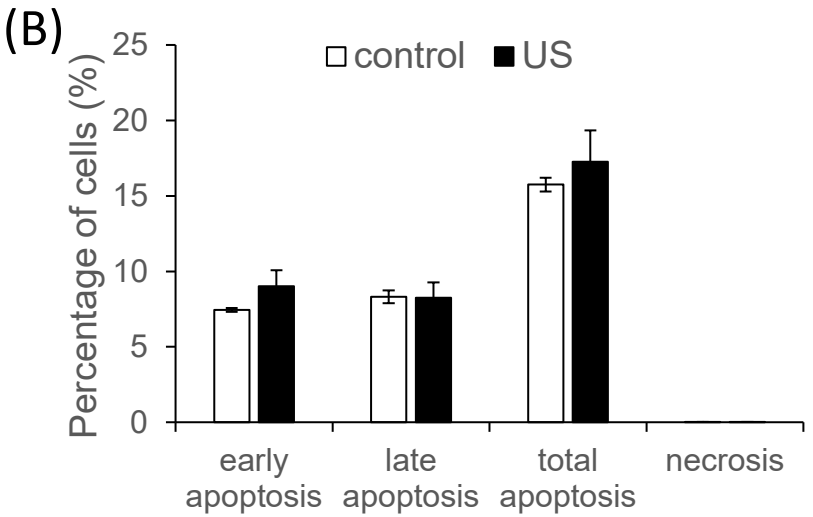

PRF: 10Hz, 24hours

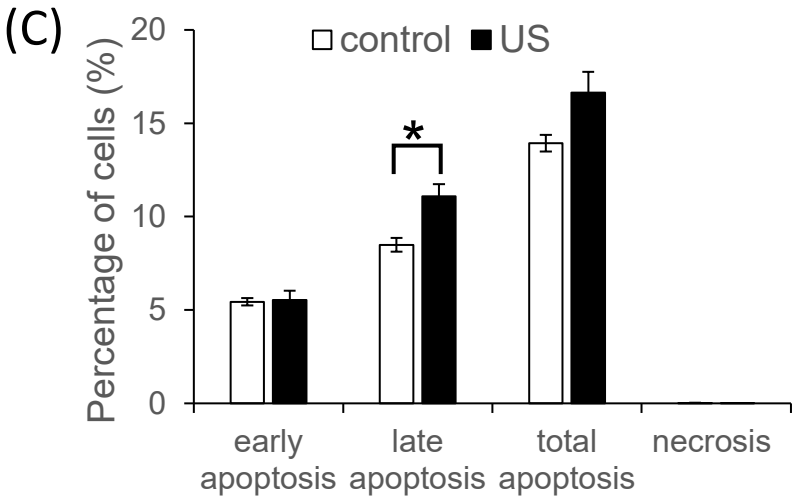

PRF: 100Hz, 0 hour

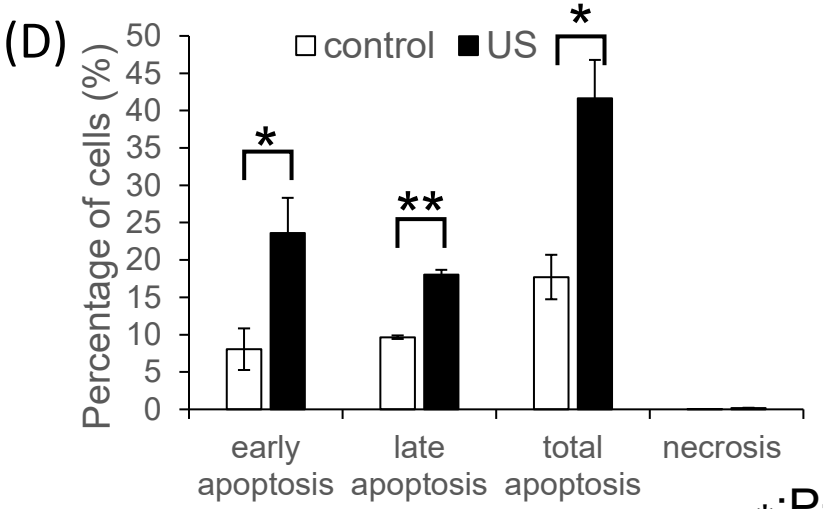

PRF: 100Hz, 24 hours

*:P<0.05

**:P<0.001

(B) PC-3

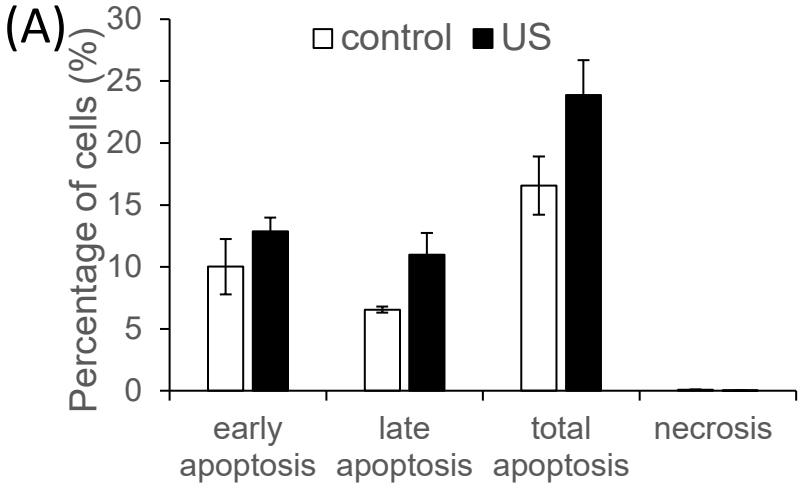

PRF: 10Hz, 0 hour

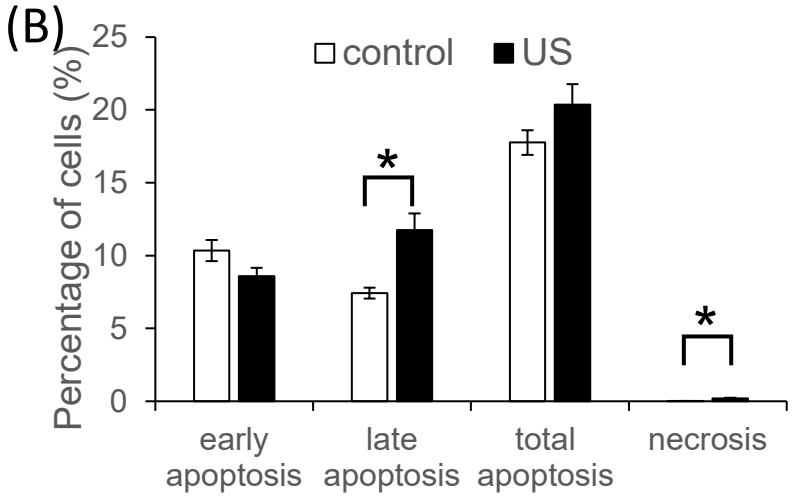

PRF: 10Hz, 24 hours

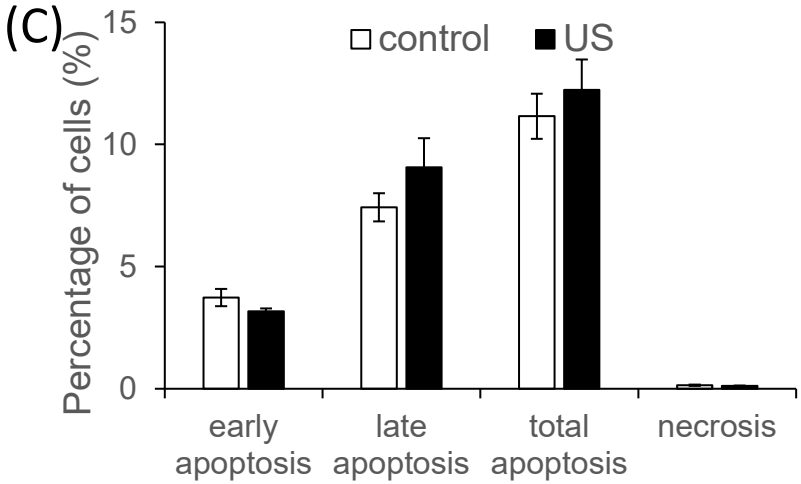

PRF: 100Hz, 0 hour

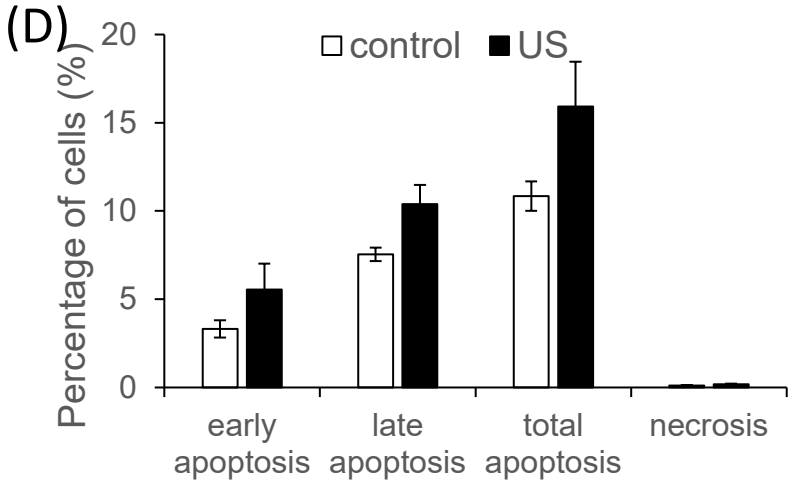

PRF: 100Hz, 24 hours

*:P<0.05

**:P<0.001

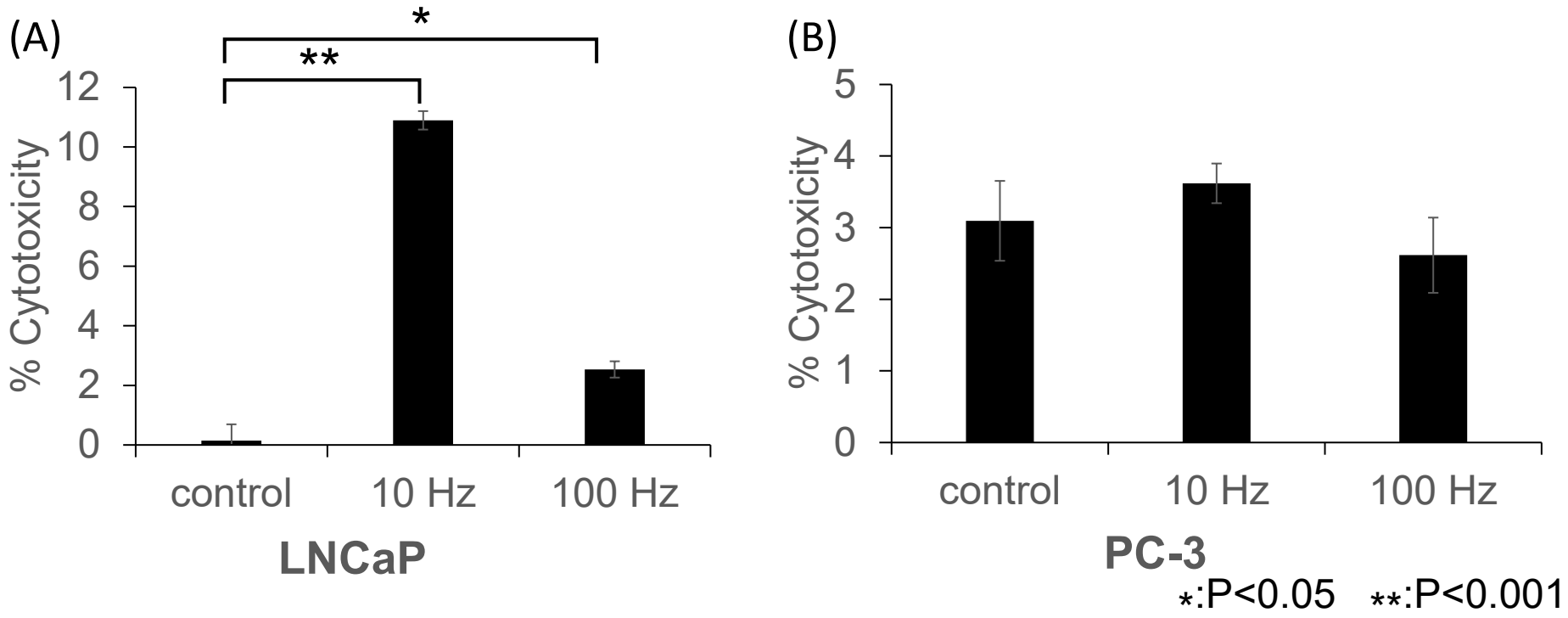
(A)
*
**
12
10
8
6
4
2
0
% Cytotoxicity
control
10 Hz
100 Hz
LNCaP
(B)
5
4
3
2
1
0
% Cytotoxicity
control
10 Hz
100 Hz
PC-3
*:P<0.05 **:P<0.001

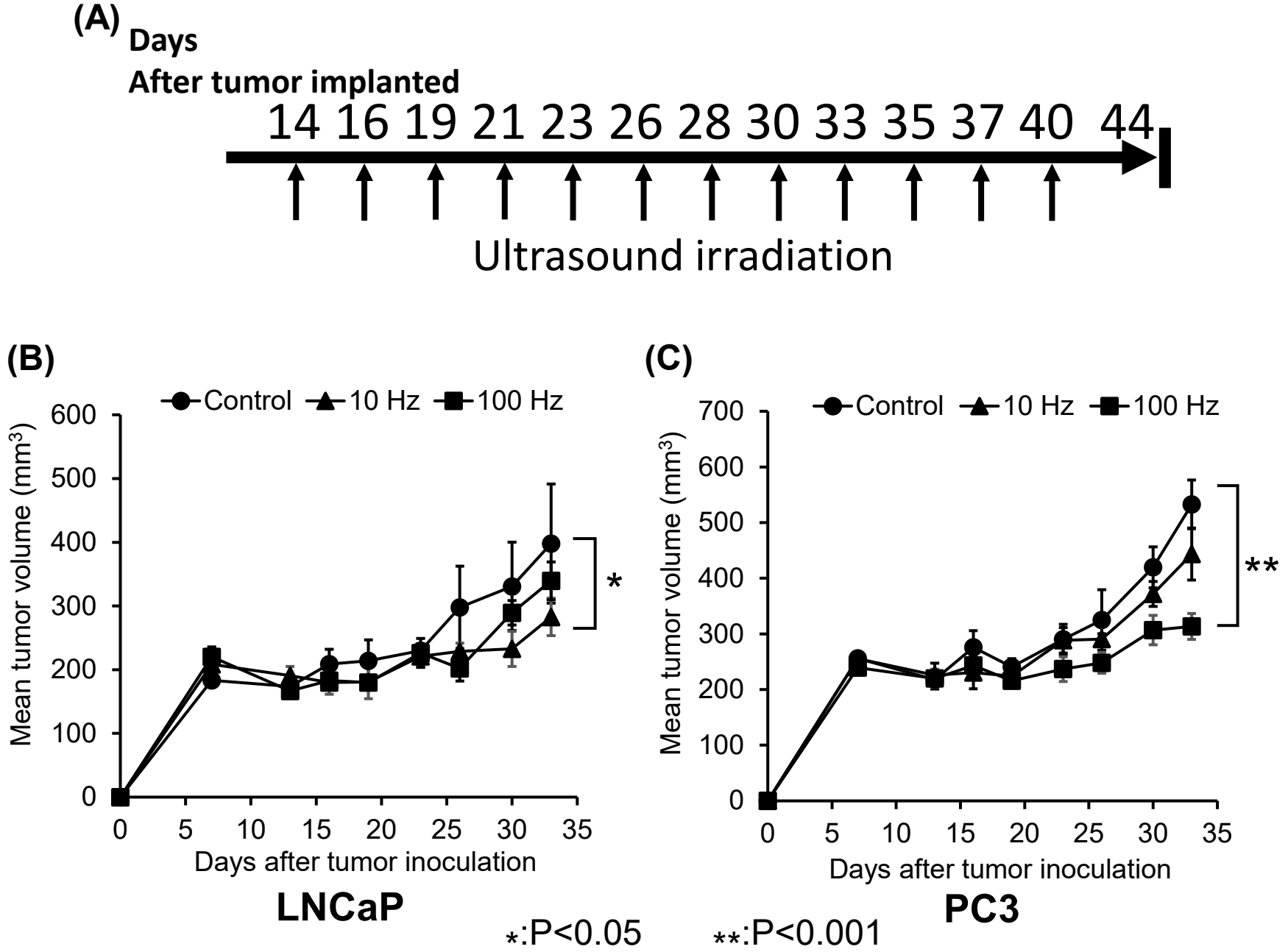
(A)
Days
After tumor implanted
14 16 19 21 23 26 28 30 33 35 37 40 44
Ultrasound irradiation
(B)
Control
10 Hz
100 Hz
Mean tumor volume (mm3)
Days after tumor inoculation
*
LNCaP
(C)
Control
10 Hz
100 Hz
Mean tumor volume (mm3)
Days after tumor inoculation
**
PC3
*:P<0.05
**:P<0.001

(A) LNCaP

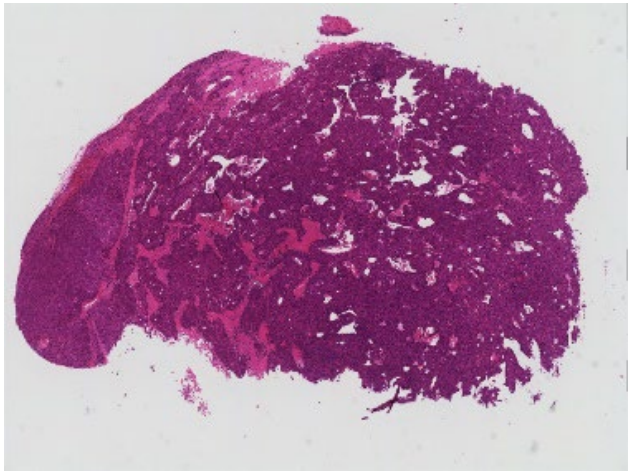

Control

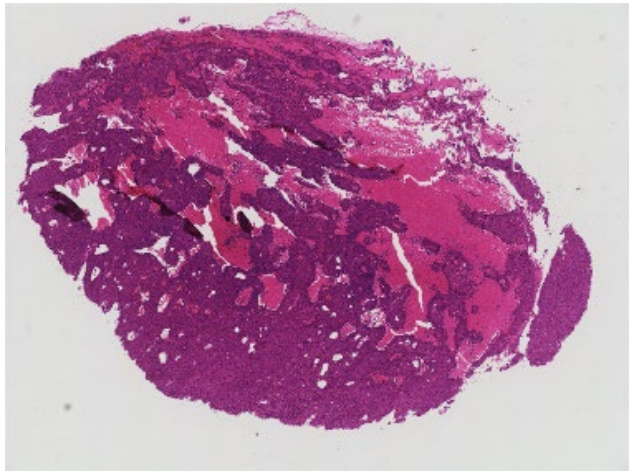

10 Hz

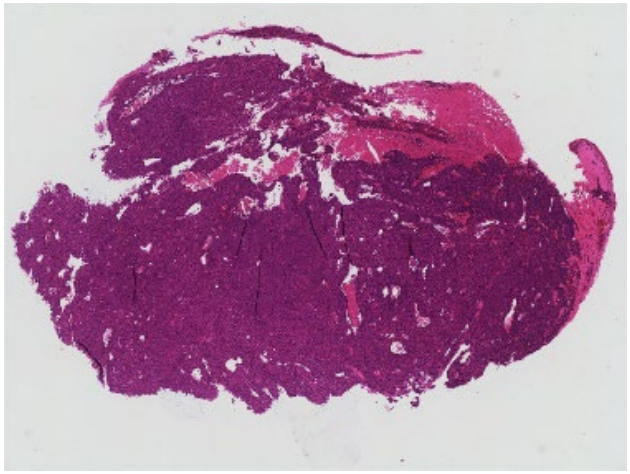

100 Hz

(B) PC-3

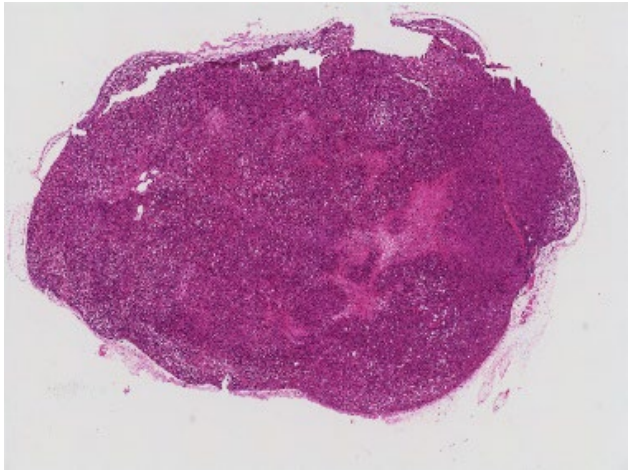

Control

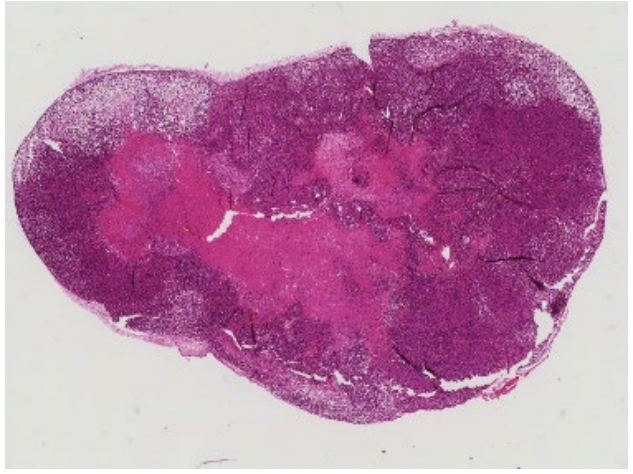

10 Hz

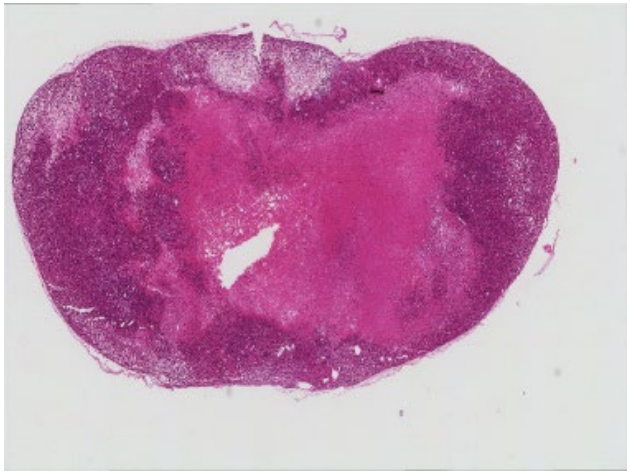

100 Hz

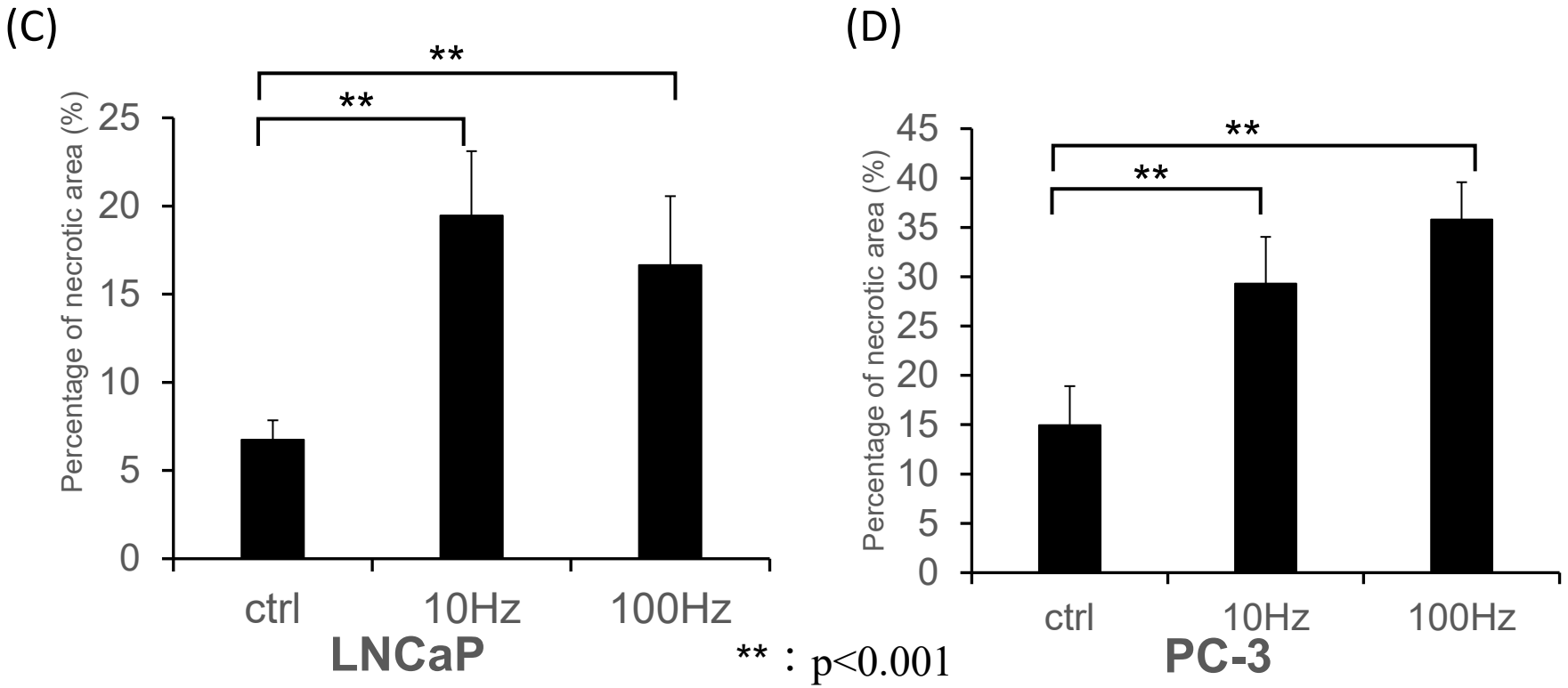
(C)
Percentage of necrotic area (%)
25
20
15
10
5
0
**
**
ctrl
10Hz
100Hz
LNCaP
(D)
Percentage of necrotic area (%)
45
40
35
30
25
20
15
10
5
0
**
**
ctrl
10Hz
100Hz
PC-3
** : p<0.001

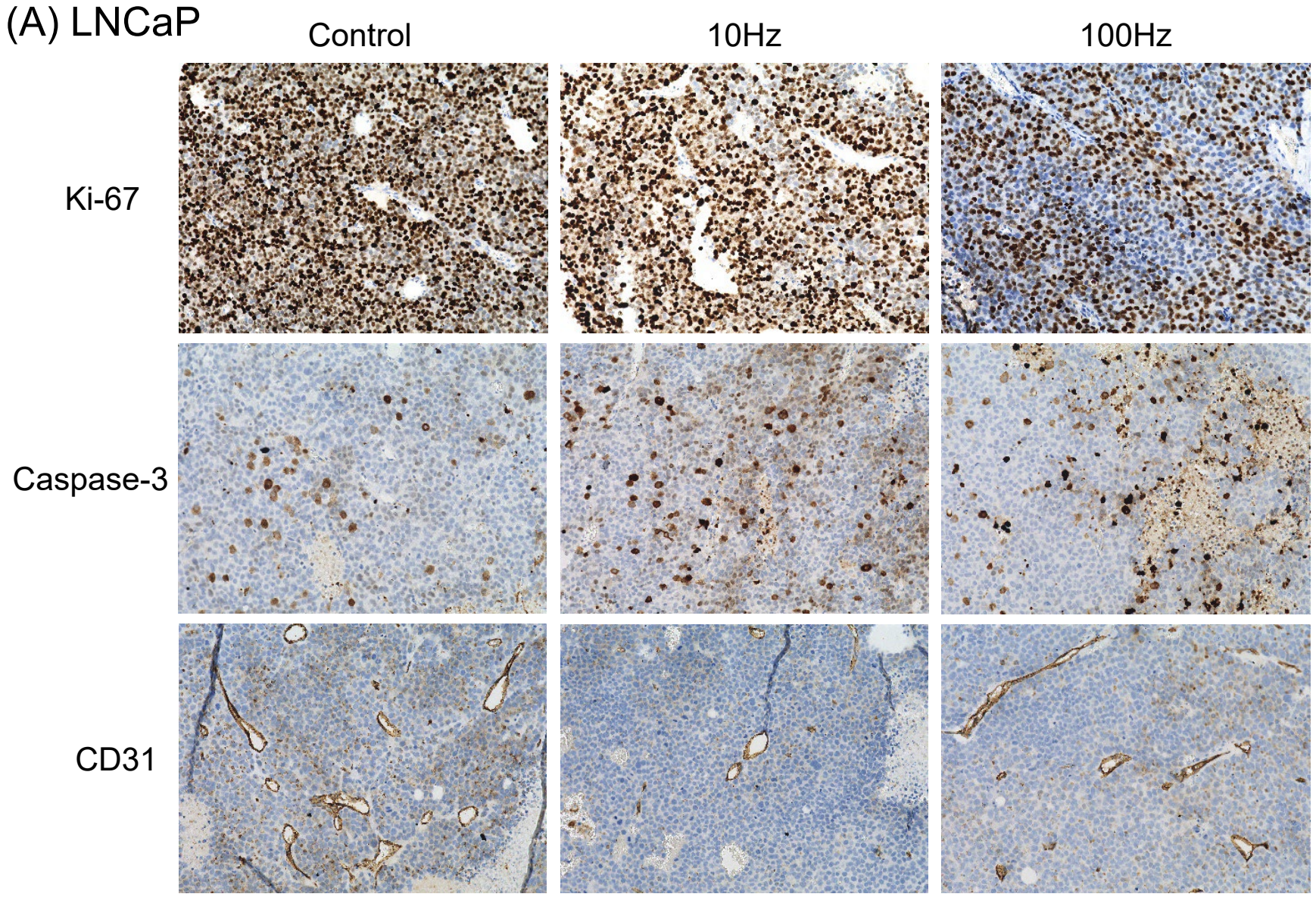
(A) LNCaP
Control
10Hz
100Hz
Ki-67
Caspase-3
CD31

(B) PC-3

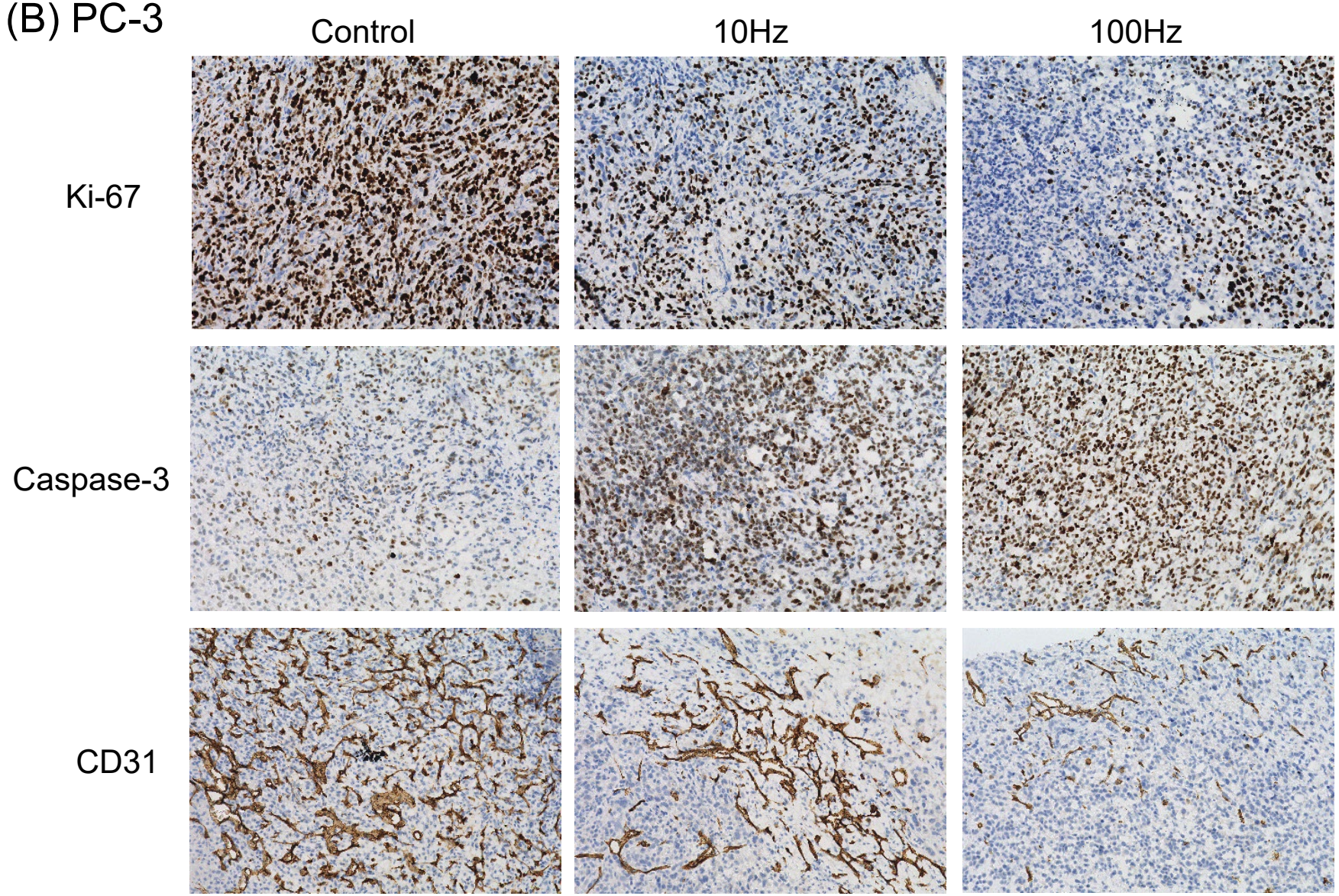

(C) LNCaP

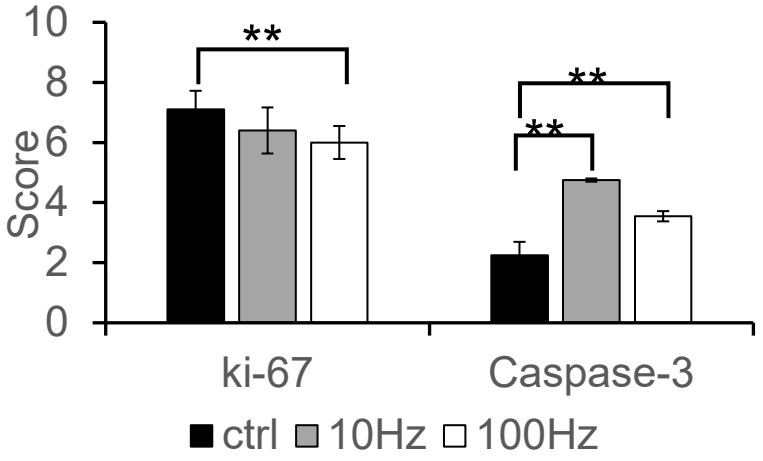

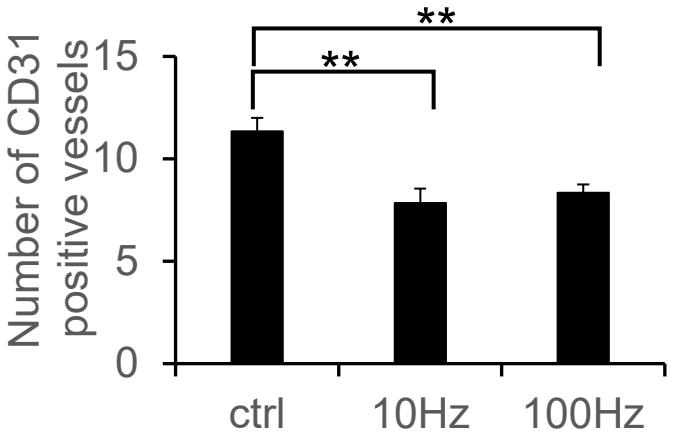

* : $p < 0.05$ ** : $p < 0.001$

(D) PC-3

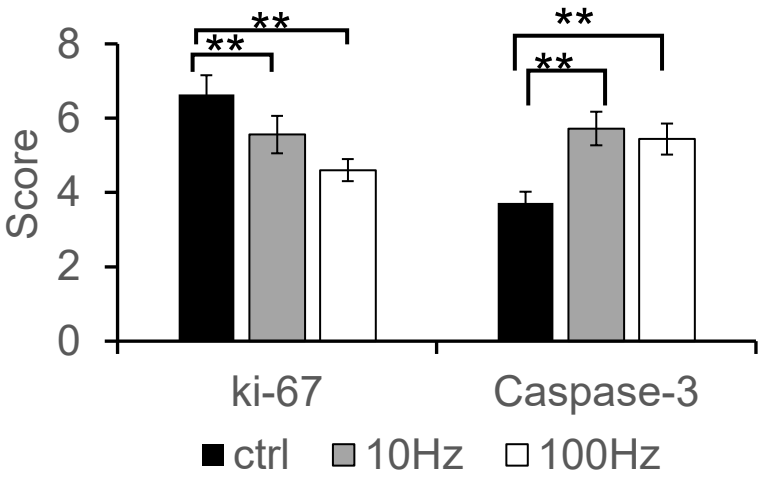

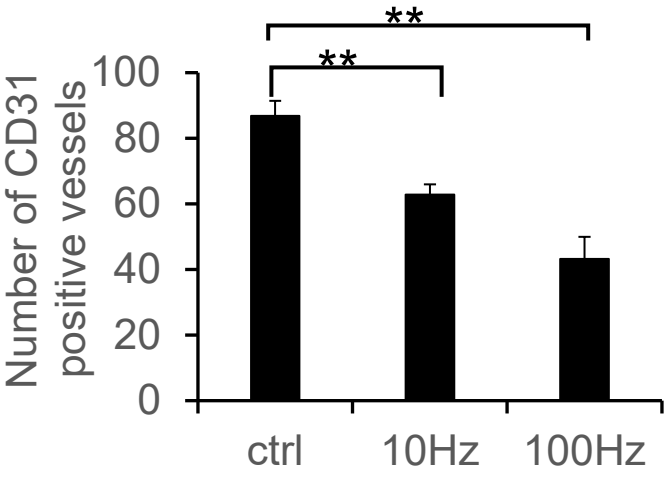

* : $p < 0.05$ ** : $p < 0.001$